
Studies on nucleic acid reassociation kinetics: V. Effects of disparity in tracer and driver fragment lengths¹

Margaret E. Chamberlin, Glenn A. Galau², Roy J. Britten³ and Eric H. Davidson⁴

Division of Biology, California Institute of Technology, Pasadena, CA 91125, USA

Received 13 March 1978

ABSTRACT

Measurements are described of the kinetics of nucleic acid strand pair reassociation where the complementary strands are of different lengths and are present in different concentrations. Rate constants for the reaction of labelled fragments ("tracer") with excess complementary strands ("driver") were determined, both for driver fragment length greater than tracer fragment length and for the reverse case. Second order reactions and pseudo-first order reactions utilizing strand separated drivers and tracers were studied. The nucleic acids which served for this investigation were ϕ X174 DNA and RNA, plasmid RSP2124 DNA and *E. coli* DNA. Approximate empirical expressions relating driver and tracer fragment lengths with the observed rate constants were obtained for practical use. In long tracer-short driver reactions the observed rate constant for the tracer reaction increases proportionately with tracer length. In long driver-short tracer reactions the rate of tracer reaction is retarded. The latter result is unexpected and appears to represent a departure from standard interpretations of the renaturation reaction.

INTRODUCTION

This paper concerns the kinetics of reactions between labelled nucleic acid fragments ("tracer") and unlabelled complementary strands of different length which are present in excess ("driver") or "short driver-long tracer" and "long driver-short tracer" reactions. Reactions of this nature are often utilized in studies of genomic sequence organization and transcriptional expression. Our main purpose is to provide empirical data from which practical kinetic predictions can be obtained. In particular it would be useful to be able to calculate approximately the rate constant for the tracer reaction in terms of the mean tracer and driver fragment lengths and the known rate constant for the driver or tracer self-reaction.

Some data concerning the rates of renaturation and hybridization between strands of different lengths are already available in the literature. Bishop et al.⁵ concluded that the length of the short strand is important in determining the rate of hybridization reactions between excess long RNA strands and short DNA tracers. Wetmur⁶ reported that in reactions between stoichiometric quantities of separated T4 DNA strands of different fragment lengths, the rate of renaturation depends essentially on the square root of the length of the shorter strand. Hutton and Wetmur⁷ showed

this is also true for reactions between ϕ X174 RNA fragments and longer DNA strands present in approximately equal amounts. However, the reactions studied by Wetmur et al. differ in two basic respects from those considered here. Our present data concern mainly reactions assayed by hydroxyapatite binding, so that the whole of any tracer molecule containing a duplex region is scored in the duplex fraction (see references 8-10 for discussion of hydroxyapatite binding as opposed to other forms of kinetic measurements). Secondly, the complementary strands are often present in very different amounts in our tracer-driver reactions. Driver/tracer mass ratios investigated in this work varied from close to unity to over 10^3 . Simple approximate relations between tracer and driver fragment lengths and the observed rate constants are suggested by the measurements we present below. However, the results are in part unexpected, and they introduce a new set of problems which require further investigation.

MATERIALS AND METHODS

Preparation, Shearing and Labelling of Nucleic Acids

RSF2124 Nucleic Acids. Plasmid RSF2124 DNA was labelled with [3 H]thymine and extracted from a bacterial lysate as described previously.¹¹ Specific activity was 1.8×10^5 cpm μg^{-1} DNA. The DNA was linearized by treatment with the restriction enzymes BamHI (New England Biolab) or EcoRI (Miles Laboratory). Strand separation was achieved by use of isopycnic CsCl gradients following denaturation of DNA for 2.5 min in 0.01 M phosphate buffer (pH 8.5), 0.001 M EDTA and reaction with an equal mass of poly(UG) (Miles Laboratory). The separated strands were further purified by renaturation and binding to hydroxyapatite. The mean length of the H-strand [3 H]DNA after hydroxyapatite purification was 4000 nucleotides (Table 1, reaction 4). The H-strand [3 H]DNA was sheared to mean lengths of 680 nucleotides by three passes at 50,000 psi through the Britten press¹² (Table 1, reaction 1); to 1100 nucleotides by a 10 sec sonication with a Bronson sonifier at setting 1 (Table 1, reaction 2); to 2400 nucleotides by sonication for 5 sec at setting 2 followed by fractionation from an alkaline sucrose gradient (Table 1, reaction 3). The 4500 nucleotide L-strand [3 H]DNA was obtained by sonication as above, followed by fractionation from a preparative alkaline sucrose gradient (Table 1, reactions 5 and 6). The 250 nucleotide L-strand [3 H]DNA was obtained by sonication for 20 sec, setting number 1 and fractionation from a preparative alkaline sucrose gradient (Table 2, reaction 1); and to 450 nucleotides by three 30 sec sonications at setting number 3 in 0.1 M NaOH (Table 2, reactions 2-5). RSF2124 [32 P]DNA (Table 1, reactions 1-4) was also labelled metabolically. The host bacteria (strain C600) were grown as usual, including chloramphenicol amplification,¹³ in L broth containing $7.5 \mu\text{Ci ml}^{-1}$ [32 P]orthophos-

phate. The DNA was extracted and purified as before.¹¹ Specific activity was 8.3×10^3 cpm μg^{-1} . The DNA was dissolved in 0.03 M Na acetate (pH 6.5), 66% glycerol. It was then sheared to 370 nucleotides mean fragment length in a Virtis homogenizer operated at 50,000 rpm for 30 min with the DNA cooled by immersion of the chamber in a dry ice acetone bath.¹² Samples of this [^{32}P]DNA were strand separated as above, and a 550 nucleotide mean fragment length (H-strand, Table 1, reactions 5 and 6) was obtained by successive fractionations from alkaline sucrose after sonication as above. The unlabelled RSF2124 DNA was also extracted, purified, and strand separated as above. H-strand fragments of mean length 7700 nucleotides (Table 2, reactions 1-5) were obtained by fractionation from a preparative alkaline sucrose gradient.

Φ X174 Nucleic Acids. Sources, procedures and methods used to obtain the Φ X174 DNA and RNA preparations used in this work (Table 2, reactions 6-9) were given in a previous publication of this series.¹⁴

E. coli DNAs. *E. coli* [^3H]DNA (Table 2, reaction 10) was labelled as follows: *E. coli* strain NB4786 was grown overnight at 37°C in L broth. [^3H]Thymine was added to a concentration of 10 $\mu\text{Ci ml}^{-1}$ and the bacteria were grown for a further 10.5 hr. The bacteria were lysed as described previously¹⁵ and the DNA was extracted according to standard procedures.¹² A final specific activity of 3×10^4 cpm μg^{-1} was obtained. The DNA was dissolved in 0.03 M NaOAc and sheared to a mean fragment length of 8330 nucleotides in a modified Virtis homogenizer at 12,000 rpm for 20 min. Unlabelled *E. coli* DNA was sheared to a mean fragment length of 700 nucleotides at 60,000 psi in the Britten press.¹² This DNA was subsequently labelled with [γ - ^{32}P]ATP at the 5' termini (Table 2, reaction 10). Details of the labelling procedure were presented earlier.¹⁵ Most of the free [γ - ^{32}P]ATP was removed from the labelled preparation by successive gel filtration through G-25 and G-50 Sephadex columns.

Other Procedures

Nucleic Acid Fragment Lengths. DNA fragment lengths were determined by velocity sedimentation analysis in alkaline sucrose gradients or by electron microscopy.^{16,17} RNA fragment lengths were determined in velocity sedimentation gradients containing formaldehyde after denaturation in the presence of formaldehyde.¹⁶ All fragment lengths cited are weight means.

Renaturation and Assay Procedures. Most of these experiments were carried out with relatively low complexity nucleic acids. The genome of RSF2124 has a complexity of about 11,300 nucleotides¹³ and that of Φ X174 has a complexity of 5374 nucleotides.¹⁸ Most of the reaction mixtures were denatured at 99°C and incubated in 0.12 M phosphate buffer, 0.2% sodium dodecyl sulfate at 60°C. In a few cases higher salt concentrations were used to accelerate the reaction at equivalent criterion conditions.¹² All values of Cot in this paper are equivalent Cot, i.e., adjusted for

the effect of salt concentrations above 0.18 M Na^+ on renaturation rate.¹² The reactions were assayed by hydroxyapatite binding at 60°C, 0.12 M phosphate buffer, 0.2% sodium dodecyl sulfate unless otherwise noted. The bound fraction was eluted at 98°C. In reaction 7 (Table 2), RNA-DNA hybrid formation was assayed by binding to hydroxyapatite at 40°C in urea phosphate.¹⁹ Radioactivity was determined for all reactions by scintillation counting.

RESULTS

Kinetics of Long Tracer-Short Driver Reactions

Strand separated RSF2124 [³H]DNA fragments of various lengths were reacted with short double and single stranded RSF2124 driver, and the kinetics of tracer duplex formation were measured by hydroxyapatite binding. Use of the strand separated tracer avoids any complication from tracer self-reaction. The first four of these reactions are shown in Fig. 1. In this series of experiments a double strand [³²P]DNA driver sheared to a mean length of 370 nucleotides was used, and tracer lengths varied from 680 to about 4000 nucleotides. The tracer-driver reactions were monitored as the fraction of the [³H]DNA bound to hydroxyapatite at each driver DNA *Cot* (closed symbols). The driver DNA self-reaction was monitored at the same time

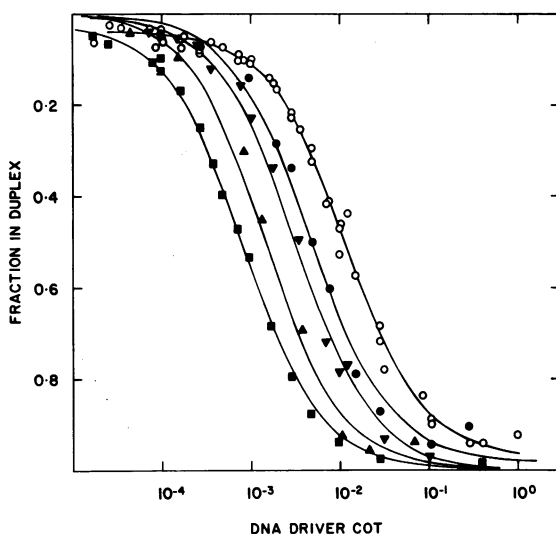


Figure 1. Kinetics of Reactions between Long Strand Separated Tracer and Short Double Stranded Driver DNAs. The driver was RSF2124 [³²P]DNA sheared to an average length of 370 nucleotides. The tracers were H-strand RSF2124 [³H]DNA sheared to mean lengths of 680 nucleotides, solid circles (●); 1100 nucleotides, solid triangles (▼); 2400 nucleotides, solid triangles (▲); and 4000 nucleotides, solid squares (■). Driver renaturation kinetics are shown by open circles (○). Reactions were assayed by hydroxyapatite binding (ordinate). The kinetics of the reactions were fit with single second order functions according to Eq. 1 (solid lines). Driver/tracer mass ratios and rate constants for these reactions are listed in Table 1 (rows 1-4).

as the bound [^{32}P]DNA (open symbols). Since both strands of the driver DNA were present, the reaction follows second order kinetics.^{10,21,22} Were the tracer the same length as the driver the reaction would be described exactly by Eq. 1:

$$\frac{T}{T_0} = \frac{1}{1 + K_T D_0 t} \quad (1)$$

Here T is the concentration of unreacted tracer DNA; T_0 is the initial tracer concentration; D_0 is the initial driver DNA concentration; K_T is the observed rate constant for the tracer-driver reaction; and t is time. As the tracer length increases relative to driver length the reaction kinetics should theoretically tend toward pseudo-first order. This is because the reaction for long tracer proceeds near to completion before the driver single strand concentration is significantly decreased. Fig. 1 shows, however, that the tracer reactions conform to second order kinetics. Thus they have been fit with Eq. 1, and the second order rate constants K_T and K_D from the experiments shown in Fig. 1 are listed in Table 1, rows 1-4. These experiments show clearly that as tracer length is increased, the rate of disappearance of totally single strand tracer fragments also increases.

Reactions 5 and 6 of Table 1 were carried out with an H-strand driver DNA. These reactions follow pseudo-first order kinetics.¹⁴ Thus the values of K_T shown in Table 1 were derived by the least squares routine assuming the relation:

$$\frac{T}{T_0} = e^{-K_T D_0 t} \quad (2)$$

Note that rate constants for pseudo-first order reactions with strand separated driver DNA are twice those for second order reactions carried out with the same nucleic acids.¹⁴ This follows from the fact that the sequence concentration is twice as high for a given mass of DNA when only one strand is present in significant quantity. Reactions 5 and 6 were identical except that 5000 nucleotide calf thymus DNA was included in a 780-fold mass excess with respect to the H-strand RSF2124 driver DNA. Table 1 shows that the value of K_T for reaction 6 is about the same as for reaction 5. The presence of a very large excess of long heterologous DNA fragments thus does not affect the kinetics of the driver-tracer reaction.

The tracer length effect on the observed kinetics of the pseudo-first order reactions is the same as on the kinetics of second order reactions. This can be seen in Fig. 2. Here we summarize the relation between tracer length and K_T , the observed rate constant for the tracer-driver reaction. The data in Fig. 2 are expressed as the ratio of K_T to the rate constant for driver reaction with complementary fragments of its own length, K_D , plotted vs. the ratio of the tracer fragment length L_T to the driver fragment length L_D . The solid line is fit through the points for reactions 1-4

Table 1. DNA Renaturation Kinetics for Long Tracer-Short Driver Reactions

| No. | Driver | L_D (NT) ^a | Tracer | L_T (NT) ^a | Driver concentration ^b ($\mu\text{g ml}^{-1}$) | Mass ratio driver/tracer | K_D ($\text{M}^{-1}\text{sec}^{-1}$) ^c | K_T ($\text{M}^{-1}\text{sec}^{-1}$) ^c | L_T/L_D | K_T/K_D |
|----------------|-----------------------------|-------------------------|---|-------------------------|--|-----------------------------|---|---|-----------|----------------|
| 1 | | | | 680 \pm 350 | 15.32, 1.593 0.1593, 0.0797 | 100 | | 209 \pm 22 (so) | 1.8 | 2.5 \pm 0.29 |
| 2 | RSF2124 double strand | 370 \pm 160 | RSF2124 H-strand [³ H]DNA | 1100 \pm 600 | 13.62, 1.416 0.1416, 0.0708 | 100 | 85 \pm 4.3 (so) | 280 \pm 33 (so) | 3.0 | 3.3 \pm 0.42 |
| 3 | [³² P]DNA | | | 2400 \pm 560 | 2.54, 0.490 0.1355, 0.0431 | 360 | | 625 \pm 131 (so) | 6.5 | 7.4 \pm 1.6 |
| 4 | | | | 4000 \pm 610 | 15.32, 4.779, 1.59x10 ⁻² 0.1593, 2.3x10 ⁻² , 7.9x10 ⁻² | 100 | | 1150 \pm 56 (so) | 11.0 | 14 \pm 1.4 |
| 5 | RSF2124 H-strand DNA | 550 \pm 175 | RSF2124 L-strand [³ H]DNA | 4500 \pm 2400 | 2.10, 2.1x10 ⁻¹ 4.02 x 10 ⁻² | 7 | (170 \pm 9) ^f (pfo) | (2040 \pm 207) ^f (pfo) | 8.2 | 12 \pm 1.4 |
| 6 ^e | | | | | 2.03, 2.08x10 ⁻¹ 4.09 x 10 ⁻² | 8.3 | | (1790 \pm 216) ^f (pfo) | 8.2 | 11 \pm 1.4 |

^aStandard deviations shown on the length estimates indicate the range in the fragment lengths obtained from the Gaussian distribution of labelled DNA in the alkaline sucrose velocity sedimentation gradients, or from measurements in the electron microscope.

^bCoat was calculated in terms of driver concentration (Eq. 1 and 2).

^cRate constants and standard deviations were calculated by use of the nonlinear least squares program for the reduction of renaturation kinetic data described earlier. The standard deviations do not include any errors which could have resulted from systematic problems with the measurements. The order of the reaction is indicated in parentheses. so, second order, fit with Eq. 1; pfo, pseudo-first order, fit with Eq. 2.

^dThe standard deviations of these ratios were calculated from the individual standard deviations listed in the preceding columns.

^eThis reaction includes a 780-fold mass excess, with respect to the H-strand driver concentration, of 5000 nucleotide-long calf thymus DNA.

^fThe driver DNA for reactions 5 and 6 was an unlabelled H-strand preparation obtained from a poly(UC) gradient (see Materials and Methods) and its purity could not be assayed directly. The kinetics of the reaction with equal length L-strand tracer were used to correct for the presence of contaminating E. coli DNA. Thus, the rate constant for this pseudo-first order reaction should be twice the rate constant for the second order reaction of double strand RSF2124 DNA of equivalent fragment length (reference 14; see text). From k_p for reactions 1-4, the pseudo-first order rate constant should be: $(85)(2) \frac{550}{370} = 207 \text{ M}^{-1}\text{sec}^{-1}$. The rate constant observed was $88 \text{ M}^{-1}\text{sec}^{-1}$. To normalize the rate constants measured to the rate constants which would have been obtained had the H-strand driver been pure, they (and their standard deviations) were multiplied by the factor $207/88 = 2.3$. The rate constants for reactions 5 and 6 are in parentheses to indicate that they are normalized rather than directly measured values. However, this correction does not affect the ratio K_T/K_D , which is the point of the experiment.

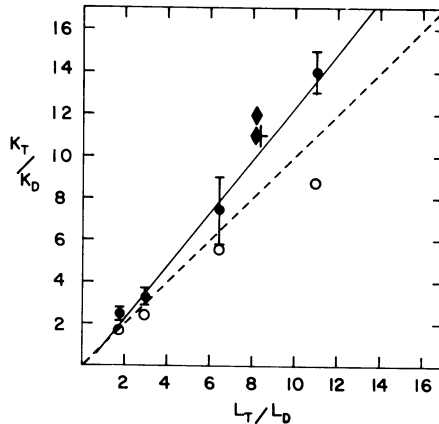


Figure 2. Rate Constants for Tracer Reactions with Shorter Drivers as a Function of Driver and Tracer Lengths. The ordinate shows the observed rate constants for the tracer reactions, normalized to the observed driver rate constant (K_T/K_D). The abscissa gives the mean tracer to driver length ratios (L_T/L_D). Data indicated by solid symbols are from Table 1 and all refer to reactions with RSF2124 DNA. Solid circles (●) indicate second order reactions (rows 1-4, Table 1) and open circles (○) are these same measurements fit with a function ("Nuform" function of ref. 20) which takes into account the fraction of the driver which remains single stranded. This function approaches pseudo-first order for long tracer/driver length ratios (see text). Solid diamonds (◆) show pseudo-first order reactions obtained with strand separated drivers (rows 5 and 6, Table 1). The cross shows a determination carried out with *E. coli* DNAs which was published earlier.²³ Error bars represent standard deviations in the rate constant ratios (Table 1). These error estimates would not include any possible systematic problems which might have affected all the determinations. The solid line represents the best least squares fit through the second order data of reactions 1-4 (Fig. 1), as these data were obtained in a single series of strand length and kinetic measurements. The dashed line is that predicted by Eq. 3 in text.

shown in Fig. 1 (solid circles). The pseudo-first order reactions (Table 1, reactions 5 and 6) are shown by the solid diamonds. Fig. 2 also contains data from an earlier publication²³ in which 4000 nucleotide *E. coli* tracer was reacted with a 450 nucleotide driver (cross). Other experiments carried out with long RNA tracers and short DNA drivers (data not shown) suggest that length effects on the observed kinetics of the tracer reaction in DNA excess RNA-DNA hybridization are similar to those obtained with long DNA tracers and short DNA drivers.

A simple empirical relation for predicting tracer rate constants for the long tracer-short driver case is suggested by Fig. 2:

$$K_T = K_D \frac{L_T}{L_D} \quad (3)$$

Here K_T and K_D are specifically the rate constants for the tracer-driver reaction and the driver self-reaction which are measured by binding to hydroxyapatite. The dashed line in Fig. 2 is that given by Eq. 3. Considering the errors in the kinetic de-

terminations and the range of the fragment lengths in the sheared preparations (Table 1), the data appear reasonably consistent with Eq. 3. Thus the small difference in slope between the line fit to the data of Fig. 1 and that generated by Eq. 3 is probably caused by a minor error in the determination of the driver length or the effect of using an approximate function for determining the rate constant. The standard deviation for the driver fragment length distribution in these experiments is about 43% (Table 1), and the results shown in Fig. 2 therefore fall well within expectations if Eq. 3 is a correct approximation. The important result shown in Fig. 2 and indicated by Eq. 3 is the linear proportionality of K_T and L_T in long tracer-short driver reactions which are assayed by the hydroxyapatite binding method.

Kinetics of Long Driver-Short Tracer Reactions

The effect of increasing driver length over tracer length is shown in a series of pseudo-first order reactions in Fig. 3. As a standard of comparison, the middle curve of Fig. 3 (solid triangles) illustrates the kinetics of the reaction of a 250 nucleotide L-strand RSF2124 [^3H]DNA tracer with excess unlabelled H-strand driver of about the same length. The 250 nucleotide L-strand tracer was also reacted with H-strand driver DNA of average fragment length 7700 nucleotides and the reaction was assayed by hydroxyapatite binding as usual. These data are indicated in Fig. 3 by the solid circles. Rate constants for this and the other reactions shown in Fig. 3 are listed in row 1 of Table 2. It is clear that the tracer-driver reaction is about 4 times slower than the reaction of the tracer with a driver of its own length. That the driver molecules actually operate as long fragments is shown in the left-most curve of Fig. 3 (solid squares). Here a reaction of the 7700 nucleotide L-strand driver with L-strand tracer almost the same length is shown. The rate constant for this reaction (K_D in Table 3) is $750 \text{ M}^{-1}\text{sec}^{-1}$ while that for the tracer fragments with complementary strands of the tracer length (K_S) is $149 \text{ M}^{-1}\text{sec}^{-1}$. Thus the ratio K_D/K_S , 5.0, is within 10% of the value predicted on the basis of the square root of the fragment lengths²⁰, $(L_T/L_D)^{1/2}$, or here 5.6. This eliminates any possibility that the long driver-short tracer reaction is retarded because of long driver degradation during the reaction. Degradation is particularly unlikely because of the low complexity of RSF2124 DNA which allows these reactions to proceed very rapidly. At the concentration used $t_{1/2}$ was about 6 min for the long driver-short tracer reaction shown.

Another possible explanation for the retardation of the tracer reaction with long driver is that the hydroxyapatite assay system fails to detect all the tracer-driver duplex formed. This might be true, for example, if the long single strand tails expected on the reacted driver molecules were to interfere with binding to the column. To check this possibility aliquots of the same reaction mixtures were digested with S1 nuclease in order to destroy the single strand tails, and were then bound to hydroxyapatite, or assayed for S1 resistance by gel filtration. Due to the fact that $L_D \gg L_T$

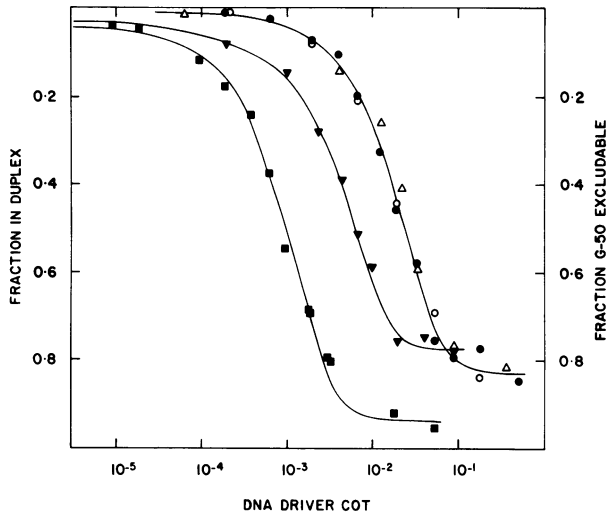


Figure 3. Retardation of Long Driver-Short Tracer Reactions. The driver DNA was unlabelled RSF2124 H-strand averaging 7700 nucleotides in length. The pseudo-first order reaction of a 7-fold excess of this DNA with a 4500 nucleotide L-strand [^3H]DNA tracer is shown by solid squares (■). A portion of the L-strand tracer was sheared to an average length of 250 nucleotides. The pseudo-first order reaction of this tracer with a 20-fold excess of H-strand driver sheared to 350 nucleotides is shown by the solid triangles (▼). The pseudo-first order reaction of the 250 nucleotide L-strand [^3H]DNA tracer with a 7-fold excess of the 7700 nucleotide driver is shown by the solid circles (●). Solid lines are best least squares solutions²⁰ according to Eq. 2. The rate constants obtained from these reactions are shown in Table 2, row 1. These three reactions were monitored directly by hydroxyapatite binding (left ordinate). Other samples of the long driver-short tracer reactions were treated with S1 nuclease. Two levels of S1 nuclease treatment were used: open circles (○) denote an S1 nuclease treatment which was partially inhibited by a low concentration of phosphate. This treatment was equivalent to an uninhibited reaction carried out at $100 \mu\text{l min mg}^{-1}$. Open triangles (△) denote treatment with $30,000 \mu\text{l min mg}^{-1}$ DNA of S1 nuclease. The light S1 treatment is sufficient to digest long single strand DNA to fragments of about 100 nucleotides in length. Reaction mixtures given the light S1 treatment were analyzed by hydroxyapatite binding (left ordinate). The heavier level of S1 treatment results in complete digestion of single stranded regions (for calibration of S1 digestion and discussion of the digestion kinetics see Britten et al.²⁴). These reactions (△) were assayed by measuring the fraction of the tracer excluded from Sephadex G-50 following the enzyme digestion.

for these reactions little S1 sensitivity of the reacted tracer should be detected (in contrast to the case for reactions between equal length fragments^{8,9}). Neither of two different S1 nuclease treatments were found to have any effect on the observed kinetics, as shown by the open symbols in Fig. 3.

In Table 2, rows 6-9, we present an additional set of experiments carried out with both double strand (RF) and (+) strand ϕX174 DNA and RNA drivers. The reaction between a randomly sheared double strand DNA and a complementary tracer of different length follows a non-second order form. The kinetics of such reactions have been

Table 2. Renaturation Kinetics for Long Driver-Short Tracer Reactions

| No. | Driver | L_D (NT) ^a | Tracer | L_T (NT) ^a | Driver conc. $\mu\text{g ml}^{-1}$ | Mass ratio driver/tracer | $K_D^{b,c}$ ($\text{M}^{-1} \text{sec}^{-1}$) | $K_S^{b,d}$ ($\text{M}^{-1} \text{sec}^{-1}$) | $K_T^{b,e}$ ($\text{M}^{-1} \text{sec}^{-1}$) | L_D/L_T | K_T/K_S^f |
|-----|---|-------------------------|---|-------------------------|---------------------------------------|-----------------------------|--|--|--|-----------|--------------|
| 1 | | | | 250 ± 110 | 13.4 | 7 | | 149 ± 8 (pfo) | 38 ± 2.5 (pfo) | 31 | 0.26 ± 0.02 |
| 2 | RSF2124 | 7700 ± 2290 | RSF2124 | | 7.97 | 3 | | | 38 ± 2.3 (pfo) | 17 | 0.17 ± 0.05 |
| 3 | H-strand DNA | | L-strand [³ H]DNA | 450 ± 200 | 16.6 | 7 | 750 ± 57 (pfo) | 32 ± 2.1 (pfo) | 32 ± 2.1 (pfo) | 17 | 0.15 ± 0.04 |
| 4 | | | | | 0.59 | 7 | | 26 ± 1.5 (pfo) | 26 ± 1.5 (pfo) | 17 | 0.12 ± 0.04 |
| 5 | | | | | 7.99 | 20 | | 36 ± 2.8 (pfo) | 36 ± 2.8 (pfo) | 17 | 0.16 ± 0.05 |
| 6 | | | $\emptyset\lambda 174$ RF [³ H]DNA | 300 ± 190 | 115.0 | 2000 | | 135 ± 22 (sc) | 55 ± 6.6 (nso) | 17 | 0.40 ± 0.08 |
| 7 | $\emptyset\lambda 174$ RF DNA | 5000 ± 200 | $\emptyset\lambda 174$ (+) strand [³² P]RNA | 360 ± 260 | 115.0 | 200 | (550 ± 30) (so) | 39 ± 5.7 (nso) | 24 ± 9.8 (nso) | 14 | 0.62 ± 0.27 |
| 8 | (+) strand $\emptyset\lambda 174$ [³² P]RNA | 1600 ± 560 | $\emptyset\lambda 174$ RF [³ H]DNA | 300 ± 190 | 0.9 | 80 | (535 ± 26) (pfo) | 199 ± 21 (pfo) | 88 ± 7 (pfo) | 5.3 | 0.44 ± 0.06 |
| 9 | (+) strand $\emptyset\lambda 174$ [¹⁴ C]DNA | 5000 ± 200 | $\emptyset\lambda 174$ RF [³ H]DNA | 300 ± 190 | 3.0 | 200 | (960 ± 50) (pfo) | 231 ± 15 (pfo) | 47 ± 6.1 (pfo) | 17 | 0.20 ± 0.03 |
| 10 | <i>E. coli</i> double strand [3H]DNA | 8330 ± 2560 | <i>E. coli</i> double strand [32P]DNA | 700 ± 295 | 512.8 | 27 | 1.51 ± .18 (so) | 0.27 ± 0.03 (so) | 0.026 ± 0.007 (nso) | 12 | 0.096 ± 0.03 |

^aStandard deviations shown on the length estimates indicate the range in the fragment lengths obtained from the Gaussian distribution of labelled DNA in the alkaline sucrose velocity sedimentation gradients, or from measurements in the electron microscope.

^bRate constants and standard deviations were calculated by use of the nonlinear least squares program for the reduction of renaturation kinetic data described earlier.²⁰ The standard deviations, of course, exclude any errors which could have resulted from systematic problems with the measurements. The order of the reaction is indicated in parenthesis. so, second order, fit by Eq. 1; pfo, pseudo-first order, fit by Eq. 2; nso, non-second order, fit by Eq. 4. To obtain the non-second order rate constants E in Eq. 4 was set at 0.5 and n at 0.45. Rate constants shown in parentheses are calculated from other data as indicated in the specific notes which follow.

^c K_p is the observed rate constant (second order, so, or pseudo-first order, pfo) for reactions of listed driver with complementary fragments of approximately equal length.

^d K_S is the observed rate constant for reactions of the listed tracer with complementary fragments of approximately equal length.

^e K_T is the observed rate constant for reactions of the tracer with complementary driver fragments of the length shown.

^fThe standard deviations of these ratios were calculated from the individual standard deviations listed in the preceding columns. Sources of rate constants and other data relevant to the individual reactions are as follows:

Reaction 1: K_p for this reaction is derived from the curve indicated by the solid squares in Fig. 3; K_S from the curve indicated by the solid triangles; K_T from the curve indicated by solid circles. Reactions 2-5: Data are from Fig. 4. K_T values are derived from the curves shown. K_D is the same as in reaction 1 (Fig. 3) and K_S is calculated by application of the square root rule.²¹ i.e., here the factor $(450/250)^{1/2}$, applied to K_S in reaction 1. In this and succeeding reactions where rate calculations were needed, standard deviations are assumed which are proportional to those measured in the reactions used for the calculation (here, e.g., K_S in reaction 1). Reaction 6: K_p for this reaction are calculated from the renaturation of 300 nucleotide RF [³H]DNA, by application of the square root rule.²¹ K_S and K_T were directly measured (data not shown). Reaction 7: K_p is the same as in reaction 6, K_T was directly measured (data not shown) and K_S was measured by Galau et al.¹¹ K_S is taken as the rate of reaction of this RNA tracer with double strand DNA fragments of similar length. This reaction is non-second order because RNA-DNA hybridization in DNA excess is slower than DNA renaturation.¹¹ The RNA-DNA reactions were assayed by the urea phosphate method of Smith et al.¹⁹ Reaction 8: K_T was measured directly (data not shown) and K_S was measured by Galau et al.¹⁴, as the pseudo-first order rate constant for reaction of RNA fragments of about equal length. K_p was calculated from data in the latter paper by application of the square root rule.²¹ The reaction was assayed by hydroxyapatite binding. Reaction 9: K_p was calculated from measurements of the pseudo-first order kinetics of the reaction between (+) strand DNA 300 nucleotides in length and a tracer of similar length, by application of the square root rule.²¹ K_S was measured by Galau et al.¹⁴ and K_T was measured directly (data not shown). Reaction 10: Rate constants listed are derived from the experiment shown in Fig. 5A. K_p is from the reaction indicated by the solid circles, and K_T from the reaction indicated by the solid triangles. K_T is the non-second order rate constant derived by application of Eq. 4. K_S for the reaction of the short [³P]DNA tracer in the absence of driver is from the curve shown in Fig. 5. Interestingly, the value of K_S for the short tracer in the presence of long driver was about half that of the free [³P]DNA tracer, as indicated in parentheses. K_S and K_p are second order rate constants obtained by application of Eq. 1.

analyzed in previous studies taking into account the fact that the tracer reacts with single strand regions of structures which also contain duplex, as well as with free driver single strands. The following relationship describes tracer reaction kinetics in this situation¹¹:

$$T/T_0 = (1 + K_D C_0 t)^{-K_T/K_D (1-E)} \exp \left(\frac{K_T E (1-[1 + K_D D_0 t])^{1-n}}{K_D (1-n)} \right) \quad (4)$$

Here T, T₀, K_T, K_D, D₀ and t are as above; E is an inhibition factor which quantitates the decreased probability of nucleation in single strand regions of driver particles also containing duplex, and n is a constant the value of which is about 0.45 (see refs. 10, 11 and 14 for derivation of this equation and relevant discussion). Eq. 4 was used to obtain those tracer rate constants in reactions 6-10 of Table 2 which are labelled non-second order (nso). By application of Eq. 4 we see that the non-second order reaction of a 5000 nucleotide double strand (RF) driver with a 300 nucleotide (RF) tracer is retarded severalfold, relative to the tracer self-reaction (Table 2, row 6), as is the pseudo-first order reaction of a 5000 nucleotide (+) strand driver with this tracer (Table 2, row 9). Similarly the pseudo-first order RNA excess hybridization reaction shown in line 8 of Table 2 occurs more slowly than do the equivalent reactions carried out with equal RNA and DNA fragment lengths (cf. Galau et al., ref. 14). However, long DNA driver-short RNA tracer reactions may represent a partial exception. One example is shown in row 7, Table 2. This non-second order reaction is retarded less than expected relative to the rate of the DNA excess hybridization measured with RNA and DNA fragments of equal length (cf. Galau et al., ref. 11). Unpublished experiments provide several other examples of relatively nonretarded DNA excess hybridizations between long RSP2124 DNAs, *E. coli* DNAs and the complementary RNAs. Interpretation of such experiments is extremely complicated, however, for the overall retardation observed is a composite of both the length effect and the little understood retardation of DNA excess hybridization observed between RNA and DNA strands of equal length.¹¹ For the present we confine to DNA-DNA renaturation and RNA excess hybridization reactions the conclusion that long driver-short tracer reactions are relatively retarded.

The retardation effects discussed so far were observed at driver-tracer mass ratios ranging from 7 to 2000. A study of the effect of varying the driver-tracer mass ratios is shown in Fig. 4. Data are listed in Table 2, rows 2-5. The same 7700 nucleotide H-strand fragments used in the experiment of Fig. 3 were reacted with 450 nucleotide L-strand tracer, and the mass ratio of H-strand to L-strand was varied from 0.3 to 20. These mass ratios could be in error by a factor of about 1.5 due to the inexactly known specific activity of the RSP2124 tracer preparations. The ratios

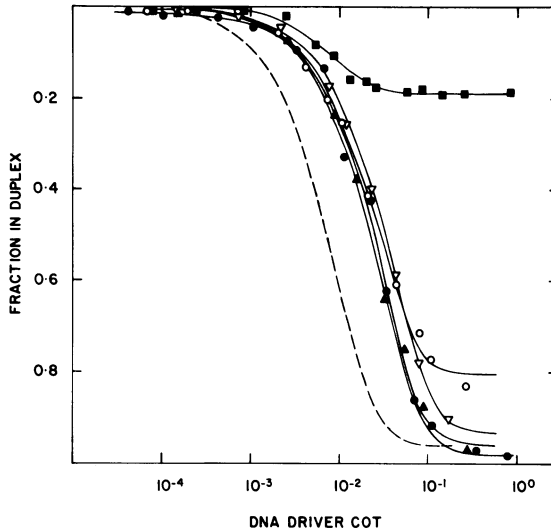


Figure 4. Effect of Long Driver-Short Tracer Mass Ratio on the Kinetics of the Tracer Reaction. The driver DNA was the same 7700 nucleotide RSF2124 H-strand preparation as used in the experiment of Fig. 3. L-strand [^3H]DNA sheared to 450 nucleotides was the tracer. The dashed line shows the kinetics of the pseudo-first order reaction of the 450 nucleotide tracer with a driver of similar length, calculated from the data of Fig. 3. Nominal mass ratios (see text) for the long H-strand to short L-strand tracer were as follows: Closed triangles (\blacktriangle), 20:1; closed circles (\bullet), 7:1; open circles (\circ), 3:1; closed squares (\blacksquare), 0.3:1. A second 7:1 driver/tracer reaction in which the absolute concentration of the driver was 28-fold lower than in the reaction denoted by closed circles is shown by open triangles (∇). All reactions were fit with pseudo-first order functions, i.e., according to Eq. 2. Driver concentrations, driver/tracer mass ratios, and pseudo-first order rate constants for these experiments are listed in Table 2, rows 2-5, with the exception of data from the tracer excess experiment. The Cot shown on the abscissa is calculated from the H-strand concentration except for the case in which the L-strand was present in excess (i.e., 0.3:1 reaction). In this case the L-strand is the driver and the Cot was calculated in terms of L-strand concentration.

cited are our best estimates derived from titration experiments in which the amount of tracer bound by known, limited quantities of driver RSF2124 DNA was measured. Our intent in the experiments of Fig. 4 is to determine at how close to a mass ratio of unity the retardation of the tracer reaction by the long driver could be observed. At a long DNA/short tracer DNA mass ratio < 1 , we expect the tracer reaction to occur at the same rate as when this tracer reacts with a driver of similar length, according to the preceding section of this paper (see Discussion). The kinetics of the reaction of the tracer with an equal length driver are shown by the dashed line in Fig. 3. However, we already know from the results shown in Fig. 3 that at long DNA/short DNA mass ratios > 7 the tracer will react more slowly. In Fig. 4 the solid squares show the kinetics of a reaction in which the mass of the short L-strand tracer was supposed to exceed the mass of the longer H-strand by a factor of about 3.3,

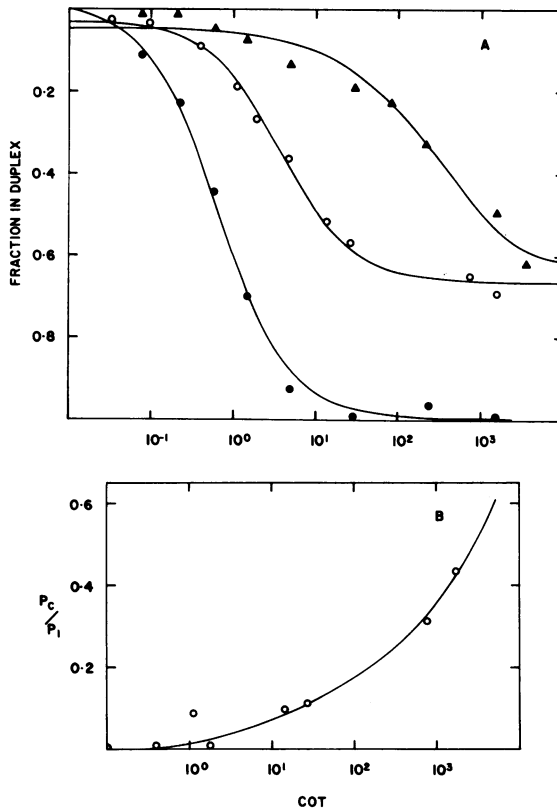


Figure 5. Renaturation of Long and Short *E. coli* DNA Fragments Assayed after Length Fractionation on Criterion CL-Sephacrose Columns. A) Kinetics of the driver self-reaction, tracer self-reaction, and driver-tracer reaction. *E. coli* [³H]DNA sheared to an average length of 8330 nucleotides was used as driver. The tracer was 700 nucleotide *E. coli* [³²P]DNA terminally labelled by the kinase procedure (see Materials and Methods). The reaction mixtures were fractionated according to particle size on CL-Sephacrose gel filtration columns operated at 60°C in 0.12 M phosphate buffer, the same criterion condition as used for the renaturation reactions. A column 28.5 x 2.5 cm was used. The 8330 nucleotide driver fragments are excluded from this column, while the tracer fragments elute as a peak with a K_{av} of 0.43. The inclusion and exclusion peaks were collected and passed over hydroxyapatite columns to determine the fraction of driver and tracer molecules which contained duplex regions. Each point analyzed contained an average of 25,000 ³H-cpm and 4000 to 8000 ³²P-cpm. Cot values plotted on the abscissa refer to the concentration of [³²P]DNA and [³H]DNA respectively for the curves describing the self-reactions, and to the [³H]DNA driver DNA concentration for the curve describing the long driver-short tracer reaction. Self-reaction kinetics for the long [³H]DNA fragments are shown by solid circles (●). Self-reaction kinetics for the [³²P]tracer, determined separately, are shown by the open circles (○). The apparent reactivity of this tracer was only 66%, due to the persistence of some free [³²P]ATP from the kinase reactions used for labelling. Reaction of the long [³H]DNA driver present in 27-fold mass excess with the [³²P]DNA tracer is shown by the solid triangles (▲). The two self-reactions are fit with second order functions. The driver-tracer reaction is fit with Eq. 4. As shown in Fig. 5B the exclusion peak of the Sepharose column includes a small frac-

tion of ^{32}P -cpm present as tracer-tracer concatenates and these must be subtracted from the total ^{32}P -cpm in the exclusion peak to determine the amount of [^3H]DNA driver- ^{32}P]DNA tracer duplex. That is, because the driver-tracer reaction is retarded, tracer self-reaction also occurs with the ultimate formation of hyperpolymers. Thus the long driver-short tracer points shown were calculated as follows:

$$P_{LS} = \frac{P_{ex} - P_H}{P - (P_I + P_H)}$$

where P_{LS} is ^{32}P -cpm in long-short duplex, P is total ^{32}P -cpm in the reaction sample, P_{ex} is total ^{32}P -cpm in duplex-containing fragments in the exclusion peak, P_H is ^{32}P -cpm in excluded tracer hyperpolymers, P_I is ^{32}P -cpm in duplex-containing fragments in the inclusion peak. P_I is thus the product of tracer self-reaction which does not exclude as hyperpolymer. $P - (P_I + P_H)$ approximately represents the single strand or available ^{32}P -tracer at each point in the reaction (actually it provides a very slight overestimate of the available ^{32}P). P_H was obtained from the values shown in Fig. 5B, normalized to the values of P_I measured directly in the driver-tracer experiment. These corrections are not exact but they are of minor significance in that they affect mainly the terminal region of the reaction, and do not at all affect the slow initial rate of the driver-tracer reaction. For example at Cot 1.5 M sec, where the tracer self-reaction is about 30% complete but the long driver-tracer reaction has scarcely begun, the values used for the calculations of P_{LS} are P_{ex} , 611 cpm; P_H , 8 cpm; P , 7864 cpm; $(P_I + P_H)$, 249 cpm. At the near terminal Cot 1660 M sec, P_{ex} is 1427 cpm; P_H , 218 cpm; P , 3156 cpm; $(P_I + P_H)$, 726 cpm. B) Hyperpolymer formation from [^{32}P]DNA self-reaction. A separate [^{32}P]DNA reaction was carried out (i.e., no [^3H]DNA fragments were present). The reactions were analyzed as in (A). Data are shown as the amount of excluded [^{32}P]DNA duplex of P_H (all excluded [^{32}P]DNA was in the duplex fraction, as expected, in both (A) and (B)), divided by the amount of [^{32}P]DNA duplex found in the included peak (P_I). Total [^{32}P]DNA Cot is shown on the abscissa, based on the optical density of the [^{32}P]DNA tracer.

according to the prior titration measurements. The terminal value obtained suggests that in fact in this experiment the short/long DNA mass ratio was about 5. Due to the low extent of the reaction a rate constant cannot be assigned with great accuracy. The best least squares solution for K_T in this reaction yields a value of $123 \text{ M}^{-1} \text{ sec}^{-1}$ (pfo rate constant calculated from the tracer concentration since it is in excess in this experiment). While perhaps a factor of two lower than the rate constant (K_S) for the tracer reaction with driver strands of equal length, this rate constant is over 3 times higher than obtained in the remaining reactions of Fig. 4, in all of which the 7700 nucleotide H-strand fragments are present in mass excess over the 450 nucleotide L-strand tracer. K_T/K_S for the latter reaction falls in the range 0.12-0.17, over a nominal driver/tracer mass ratio range of 3 (row 2) to 20 (row 5). Decrease of absolute driver concentration by a factor of 28 (Table 2, rows 3 and 4) does not significantly alter the results. The absolute driver concentrations in the RSF2124 reactions fall in the same range as the driver concentration in the $\text{OX}174$ experiments discussed above (rows 6-9 in Table 2). We conclude that at least at total nucleic acid concentrations over $0.5 \mu\text{g ml}^{-1}$ the decrease in the rate of the tracer reaction with long complementary driver DNA occurs when the driver/tracer mass ratios are as low as 3 to 5. Note that the ratio of long to short fragments by count is still in

favor of the tracer at these mass ratios and lengths. Fig. 4 and Table 2 show furthermore that no additional retardation occurs as the driver/tracer mass ratio is increased.

An independent demonstration of the long driver-short tracer retardation is shown in Fig. 5. Here we have utilized a size separation method to isolate long driver-short tracer reaction products so that they can be observed directly. Excess *E. coli* [^3H]DNA driver about 8330 nucleotides long was reacted with [^{32}P]DNA tracer fragments averaging 700 nucleotides. The reaction mixtures were passed over a cross-linked Sepharose gel filtration column operated at the same criterion condition (60°C , 0.12 M phosphate buffer) as used for the renaturation reactions. The exclusion peak contains [^3H]DNA driver- ^{32}P]DNA tracer duplexes, and any [^{32}P]DNA hyperpolymers which attain large size. The inclusion peak contains only tracer molecules. Both exclusion and inclusion peak fractions were analyzed for duplex content by hydroxyapatite binding. Fig. 5A displays the kinetics of the driver self-reaction, the tracer self-reaction, and the driver-tracer reaction. In Fig. 5B the rate of tracer hyperpolymer formation is shown. The definition of hyperpolymer afforded by this experiment is of course arbitrary. Probably at least 4 tracer fragments are required for exclusion from the CL-Sepharose column, and the rate of hyperpolymer accumulation is no doubt affected by strand scissions. The quantity of hyperpolymers in the exclusion peak must be subtracted from the total [^{32}P]DNA in duplex found there, if one is to obtain an accurate estimate of the driver-tracer duplex content. We utilized the data of Fig. 5B to make this correction.

The rate constants for the three reactions shown in Fig. 5A are listed in row 10 of Table 2. It is again evident that a large retardation occurs when the tracer reacts with the longer driver, compared with its self-reaction. This retardation is observed in the initial phase of the reactions as well as later, and even at the beginning the reaction proceeds at least threefold more slowly than does the tracer self-reaction. The retardation obtained from the curve fit to the overall data shows close to a tenfold retardation. The reaction slows down progressively, possibly due to interference from large complex structures found during the later phases of driver renaturation.

Though only a limited number of reactions have been examined (Table 2), we can obtain a rough estimate of the relation between the driver/tracer length ratio and the observed tracer rate from the data in Table 2. In the last column of Table 2 the rate constant for the tracer reaction with long driver (K_T) is compared to the rate constant for the tracer reaction with complementary fragments of equal length (K_S). A plot of K_T/K_S vs. L_D/L_T is shown in Fig. 6. The data are somewhat scattered, which is not greatly surprising considering the fact that both parameters plotted are ratios of values each of which has a certain range (see Table 2), and that data from several different nucleic acid systems are pooled. The solid line shows the value of K_T/K_S if the observed tracer rate were to vary as $(L_D/L_T)^{1/2}$. The data are not

obviously inconsistent with this assumption, but appear to be inconsistent with the alternative that K_T/K_S varies as $(L_D/L_T)^{-1}$. Thus for empirical calculations we suggest that in long driver-short tracer reactions the tracer rate constant can be conveniently calculated as follows:

$$K_T = K_S \left(\frac{L_T}{L_D} \right)^{1/2} \quad (5)$$

We stress that Eq. 3 and Eq. 5 are meant only for the practical purposes of calculating expected tracer rate constants within the accuracy of most experiments. Since different functions cannot govern the rate of tracer reaction for $L_T > L_D$ and $L_T < L_D$, Eq. 3 and Eq. 5 cannot be correct in detail. Though a more complex function of L_D and L_T can be derived which will provide a smooth transition through the region

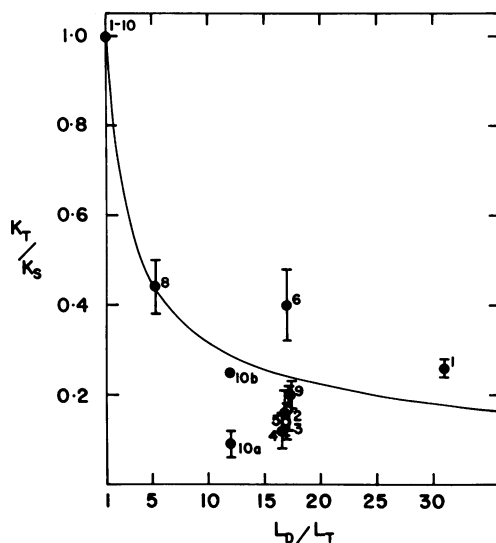


Figure 6. Retardation of Tracer-Driver Reactions as a Function of Driver and Tracer Fragment Lengths. Data are from Table 2, and are keyed numerically to indicate the source of each point in Table 2. K_T is the observed rate constant for the reaction of the short tracer with longer driver fragments, K_S is the observed rate constant for the reaction of tracer with fragments of approximately the same length, and L_D and L_T are the mean driver and tracer fragment lengths, respectively. Both pseudo-first order and second order reactions are shown. An RNA excess hybridization is plotted (reaction 8), but no DNA excess RNA hybridization reaction is included since the kinetics of these reactions are additionally complex (see text). The point labelled 10 a, from the experiment of Fig. 5A, shows the best overall non-second order rate constant, derived as indicated in Table 2, row 10. The point labelled 10b is our best estimate of the rate constant for the initial phase of the reaction, calculated from the first four points of the driver-tracer reaction shown in Fig. 5A. This is clearly a minimum estimate of the relative retardation of the long driver-short tracer reaction but it shows that the reaction begins at a rate at least 3-fold slower than the rate of the tracer self-reaction. The ordinate intercept, labelled "1-10", is by definition the rate of the tracer reaction with fragments of equal length normalized to itself, or unity. The solid line drawn through the points is the function generated by Eq. 5 in text.

where $L_D = L_T$ and which will also approximate Eq. 3 where $L_T \gg L_D$ and Eq. 5 where $L_D \gg L_T$, no significant gain in accuracy or understanding is thus achieved.

DISCUSSION

The results presented in this paper provide convenient approximate formulae useful for experimental calculations, but they also raise an interesting issue in renaturation kinetics. This can be most simply stated as follows. In long tracer-short driver reactions the nucleation rate for the short molecules is the same as when these short molecules are reacting with complementary fragments of the same length. However, when the excess nucleic acid is longer than the tracer, the nucleation rate for the short molecules falls as a function of the driver length, and the tracer reaction is retarded. Therefore the nucleation rate for the short molecules depends on their concentration relative to that of the long molecules. This represents a deviation from the basic paradigm suggested by the approximately second order kinetics of DNA renaturation, viz. that there is a nucleation rate constant which depends only on the length and complexity of the interacting strand pairs, and the external nature of the environment (ionic strength, viscosity, temperature, etc.). The unexpected retardation we observe occurs in reactions where only one driver strand is present and in reactions where both are present. Therefore, interference from the complementary driver strand is not an explanation. The experiment in which long calf thymus DNA was present in excess (Table 1, reaction 6) shows furthermore that addition of heterologous nucleic acids to the solution has no discernable effect on the kinetics of the driver-tracer reaction. Thus it is the excess concentration of complementary long driver strands which slows the tracer reaction.

We now briefly review the specific arguments leading to the paradoxical conclusion that the nucleation rate for the short fragments depends on the relative concentrations of long driver fragments. In long tracer-short driver reactions the observed rate of tracer reaction increases proportionately with tracer length, as stated by Eq. 3. It follows from this that the nucleation rate for short strands reacting with longer tracer fragments remains the same as when the short strands react with complementary fragments of similar length. This can be seen by considering the factors which enter into the observed rate constant. If hydroxyapatite binding is used to monitor the reaction, the whole of any molecule containing a duplex region is scored as having reacted. Therefore the yield for each successful nucleation is L nucleotides, where L is the length of the fragment. The observed rate constant for the reaction of driver molecules with complementary molecules of equal length, K_D , can thus be expressed in terms of the yield per nucleation and the probability of nucleation, as shown earlier (see the studies of Wetmur and Davidson²¹ and Wetmur⁶ on length dependence of nucleation rate; and Britten and Davidson¹, particularly Eq. 4 of the

latter paper and ancillary discussion):

$$K_D = \left(\frac{K_n}{L_D^{1/2}} \right) L_D = K_n L_D^{1/2} \quad (6)$$

Here K_n is a relative length-independent constant which expresses the rate of nucleation per nucleotide, and which depends on nucleic acid complexity as well as on the external conditions. Thus $K_n/L_D^{1/2}$ expresses the observed decrease in the rate of nucleation at any given nucleotide with increasing chain length. Since the yield of the reaction as measured by hydroxyapatite binding increases with chain length, an overall $L^{1/2}$ dependence is observed for the empirical rate constant for driver renaturation.²¹ Now suppose we react the same driver with a longer tracer and we continue to measure the tracer reaction by hydroxyapatite binding. If the nucleation rate of the short driver molecules does not change, only the yield is altered, and the observed rate constant K_T would be expressed:

$$K_T = \left(\frac{K_n}{L_D^{1/2}} \right) L_T \quad (7)$$

Thus K_T would vary as L_T , and if we divide (Eq. 7) by (Eq. 6), we have

$$\frac{K_T}{K_D} = \frac{L_T}{L_D} \quad (8)$$

Eq. 8 is the same as Eq. 3 and is the relation followed approximately by the data (Fig. 2). Thus, in long tracer-short driver reactions the nucleation rate for the short molecules appears to remain the same as when they are reacting with complementary molecules of equal length.

On the other hand, the presence of excess long driver lowers the rate of successful nucleation with short strands. This follows directly from the results presented in Fig. 3-6 and in Table 2. The relative nucleation rate constants (J) are calculated explicitly in Table 3. We define a relative nucleation rate constant, J , which consists of the observed rate constant, K_T , divided by the yield per nucleation (see analogous expression in Eq. 6):

$$J = \frac{K_T}{L_T} \quad (9)$$

For any pair of fragments J should remain constant, regardless of which is labelled and which is in excess. It can be seen that J remains approximately constant for the long tracer-short driver reaction, and these values are about equal to the value of J in the reaction of the tracer with complementary fragments of the same length.

Table 3. Nucleation Rate for Shorter Fragment in Long Driver-Short Tracer Reactions

| 1 Nucleic Acid | 2 Reaction | 3 Data | 4 L_T | 5 L_D | 6 K_T | 7 Relative Nucleation Rate Constant (J) | 8 Order |
|---------------------------------|---------------------------------|------------------------|------------|------------|------------|---|------------|
| RSP2124 DNA | equal length driver & tracer | Table 1, reactions 1-4 | 370 | 370 | 85 | 0.23 | so |
| | long tracer- short driver | Table 1, reaction 1 | 680 | 370 | 209 | 0.31 | so |
| | | Table 1, reaction 2 | 1100 | 370 | 280 | 0.25 | so |
| | | Table 1, reaction 3 | 2400 | 370 | 625 | 0.26 | so |
| | | Table 1, reaction 4 | 4000 | 370 | 1150 | 0.29 | so |
| | equal length driver & tracer | Table 2, reaction 1 | 250 | 250 | 149 | 0.60 | pfo |
| | | Table 2, reactions 2-5 | 450 | 450 | 220 | 0.49 | pfo |
| | long driver- short tracer | Table 2, reaction 1 | 250 | 7700 | 38 | 0.15 | pfo |
| | | Table 2, reaction 2 | 450 | 7700 | 38 | 0.08 | pfo |
| | | Table 2, reaction 3 | 450 | 7700 | 32 | 0.07 | pfo |
| | | Table 2, reaction 4 | 450 | 7700 | 26 | 0.06 | pfo |
| | | Table 2, reaction 5 | 450 | 7700 | 36 | 0.08 | pfo |
| ØX174 RNA (ex- cess) and DNA | equal length driver & tracer | Table 2, reaction 8 | 300 | 300 | 199 | 0.66 | pfo |
| | | Table 2, reaction 9 | 300 | 300 | 231 | 0.77 | pfo |
| ØX174 DNA | long driver- short tracer | Table 2, reaction 8 | 300 | 1600 | 88 | 0.29 | pfo |
| | | Table 2, reaction 9 | 300 | 5000 | 47 | 0.16 | pfo |

Representative data from Tables 1 and 2 are used as indicated in column 3. Data shown include all the pseudo-first order and second order reactions from Tables 1 and 2, i.e., excluding reactions 6, 7 and 10 of Table 2 and also reactions 5 and 6 of Table 1, which are redundant. For a given nucleic acid, pseudo-first order (pfo) reaction rate constants are expected to be about 2 times higher than second order reaction rate constants (so), as noted in Results. This relation can be seen clearly in comparing the relative pfo and so nucleation rate constants for the equal length reactions of RSP2124 DNA. Due to its lower complexity, the relative nucleation rate constant for ØX174 reactions should be about twofold higher than those for RSP2124, but a difference of only about 1.5 is observed, using the average nonretarded values of J listed in column 7 and correcting for the small length differences. This deviation is within error. J is calculated as shown in Eq. 9 of text.

However, when the driver is longer, the relative nucleation rate constant J for the short tracer fragment decreases sharply. The decrease in J as driver length increases relative to a given tracer length means that the basic rate of nucleation per nucleotide in the short fragment is lowered by the presence of the excess long strands.

The retardation of long driver-short tracer reactions is the second example of deviation from expected behavior uncovered in our recent investigations of renaturation kinetics. A somewhat similar kinetic asymmetry was seen by Galau et al.^{11,14} who showed that while RNA excess hybridization with DNA occurs at about the rate of DNA renaturation, DNA excess hybridization with RNA is retarded about 3- to 4.5-fold. As in our present case the latter phenomenon is observed in pseudo-first order as well as second order reactions and is not affected by heterologous nucleic acids.

The retardation of the driver-tracer reaction in the presence of excess long driver may imply the existence of transient but sequence-specific interactions between complementary strands. Perhaps such interactions temporarily trap the short molecules in conformations which decrease the probability of fruitful nucleations or retard zipping. The experiment of Fig. 5 did not detect the presence of such complexes, however. In any case, since the retardation phenomenon depends on excess long strands in the concentration range we have studied, it should disappear at low nucleic acid concentrations and perhaps under different ionic or temperature conditions or in different solvents. It would clearly be informative to determine the conditions in which ideal behavior is observed, in the sense that the nucleation rate for the reaction of long with short molecules would depend only on the characteristics of the reacting strand pairs and would be independent of their relative concentrations.

ACKNOWLEDGMENTS

The authors gratefully acknowledge the gifts of ϕ X174 nucleic acids by Drs. Lloyd H. Smith, Amy S. Lee, Paul A. Johnson, and Robert L. Sinsheimer. We thank Drs. Robert C. Angerer and Terry L. Thomas and Mr. Cary Lai for their assistance in preparing some of the other nucleic acids used in this study. It is a pleasure to acknowledge the contribution of Dr. Michael J. Smith, then of this laboratory, who performed the initial experiments on tracer reaction rates in the presence of longer drivers. Professor Norman Davidson, Dr. Terry Thomas, and Mr. Frank Costantini provided extremely useful critical reviews of the manuscript. This research was supported by an NIH Grant GM20927.

REFERENCES

- 1 Papers No. I, II, III, and IV in this series are respectively references 9, 10, 14, and 11 below
- 2 Present address: Department of Biochemistry, University of Georgia, Athens, GA 30601
- 3 Also Staff Member, Carnegie Institution of Washington. Address: Kerckhoff Marine Laboratory, California Institute of Technology, 101 Dahlia Street, Corona del Mar, CA 92625
- 4 To whom requests for reprints should be addressed
- 5 Bishop, J. O. (1975) *Phil. Trans. Roy. Soc. B* 272, 147-157
- 6 Wetmur, J. G. (1971) *Biopolymers* 10, 601-613
- 7 Hutton, J. R. and Wetmur, J. G. (1973) *J. Mol. Biol.* 77, 495-500
- 8 Morrow, J. (1974) Ph.D. Dissertation, Stanford University
- 9 Smith, M. J., Britten, R. J. and Davidson, E. H. (1975) *Proc. Nat. Acad. Sci., USA* 72, 4805-4809
- 10 Britten, R. J. and Davidson, E. H. (1976) *Proc. Nat. Acad. Sci., USA* 73, 415-419
- 11 Galau, G. A., Smith, M. J., Britten, R. J. and Davidson, E. H. (1977) *Proc. Nat. Acad. Sci., USA* 74, 2306-2310
- 12 Britten, R. J., Graham, D. E. and Neufeld, B. R. (1974) in *Methods in Enzymology*, Vol. 29, Part E, pp. 363-418. Academic Press, New York
- 13 So, M., Gill, R. and Falkow, S. (1975) *Mol. Gen. Genet.* 142, 239-249

- 14 Galau, G. A., Britten, R. J. and Davidson, E. H. (1977) *Proc. Nat. Acad. Sci., USA* 74, 1020-1023
- 15 Scheller, R. H., Thomas, T. L., Lee, A. S., Klein, W. H., Niles, W. D., Britten, R. J. and Davidson, E. H. (1977) *Science* 196, 197-200
- 16 Davidson, E. H., Hough, B. R., Klein, W. H. and Britten, R. J. (1975) *Cell* 4, 217-238
- 17 Chamberlin, M. E., Britten, R. J. and Davidson, E. H. (1975) *J. Mol. Biol.* 96, 317-333
- 18 Barrell, B. G., Air, G. M. and Hutchison, C. A. (1976) *Nature* 264, 34-41
- 19 Smith, M. J., Chamberlin, M. E., Hough, B. R. and Davidson, E. H. (1974) *J. Mol. Biol.* 85, 103-126
- 20 Pearson, W. R., Davidson, E. H. and Britten, R. J. (1977) *Nucleic Acids Res.* 4, 1727-1737
- 21 Wetmur, J. G. and Davidson, N. (1968) *J. Mol. Biol.* 31, 349-370
- 22 Britten, R. J. and Kohne, D. E. (1968) *Science* 161, 529-540
- 23 Davidson, E. H., Hough, B. R., Amenson, C. S. and Britten, R. J. (1973) *J. Mol. Biol.* 77, 1-23
- 24 Britten, R. J., Graham, D. E., Eden, F. C., Painchaud, D. M. and Davidson, E. H. (1976) *J. Mol. Evol.* 9, 1-23